A Thermal Broadening Study of the Antenna Chlorophylls in PSI-200, LHCI, and PSI Core

Roberta Croce,‡ Giuseppe Zucchelli, Flavio M. Garlaschi, and Robert C. Jennings*

Centro C.N.R. Biologia Cellulare e Molecolare delle Piante, Dipartimento di Biologia, Università di Milano, Via Celoria 26, 20133 Milano, Italy

Received June 4, 1998; Revised Manuscript Received August 5, 1998

ABSTRACT: The intact photosystem I of maize containing its full antenna complement (PSI-200) has been purified and fractionated into the core and outer antenna (LHCI) components. It is demonstrated by absorption and fluorescence spectroscopy that at least 80% of the long wavelength absorbing antenna pigments (red forms) are located in LHCI. Absorption spectra in the Q_y region of all three preparations were measured between 72 and 300 K and subjected to a thermal broadening analysis. Data are interpreted in the linear electron−phonon coupling assumption, and the average optical reorganization energy ($S\nu_m$) for the bulk pigment band and the red absorption tail determined. A marked asymmetry in $S\nu_m$ values across the absorption band is demonstrated. The bulk pigments in all three preparations have rather low values, in the range of 15−25 cm^{-1}, suggesting that Stokes shifts for the absorption forms are in the 1.5−3 nm range. On the other hand the red forms have markedly greater reorganization energies. While a direct thermal analysis of the red tail indicates minimum $S\nu_m$ values of around 60 cm^{-1}, when the contribution of the red tail of the bulk pigments is corrected for in LHCI, the more reliable value of 110 cm^{-1} is obtained. These high $S\nu_m$ values for the red pigment forms suggest that they have unusually wide homogeneously broadened absorption bands and large Stokes shifts (6−11 nm).

It has long been recognized that the antenna of higher plant photosystem I possesses unusual spectroscopic properties associated with the presence of significant absorption in the long wavelength tail (e.g., ref *1*−*3*) which is due to the presence of a number of chlorophyll spectral forms absorbing at energies which are lower than that of the primary photochemical trap, P700. These red forms account for 5−7% of the total PSI absorption. It was initially thought that their excited states become significantly populated only at cryogenic temperatures (e.g., refs *4*, *5*), which apparently obviated the problem of uphill energy transfer to P700. However more recently it has been clearly demonstrated, using both steady-state and time-resolved techniques, that the fluorescence emission is in fact dominated by the red forms at room temperature (*6*, *7*). Furthermore it was shown for maize PSI-200 (*7*), and more recently for the *Synechococcus* PSI core (*8*), that the room-temperature fluorescence spectrum can be almost exactly calculated from the absorption spectrum using the Stepanov expression (*9*) which assumes thermal equilibration of excited states between all energy levels in the system. These studies demonstrate that about 85% of the room-temperature excited-state population is associated with the red forms and underline their importance in energy transfer processes in PSI antenna. While it has been suggested that the low-energy forms may serve to increase the rate of energy flow from the antenna by focusing energy on the reaction center (*10*) most opinion, based on model studies, suggests that they do in fact slow down this process (*11*−*13*), due to the fact that they are energetically much lower than P700 (1−3 kT at room temperature). The possibility that they may significantly increase the absorption cross section of PSI in certain environmental conditions has been suggested (*12*, *14*).

Despite considerable experimental effort, progress in understanding the detailed spectroscopic properties of the red forms has been rather slow, mainly due to the lack of absorption structure in the red tail. The strong fluorescence signal, however, has permitted identification of two red emitting pigment pools near 720 and 735 nm (*1*, *15*−*17*) though the 735 nm emission was recently demonstrated to be heterogeneous in maize PSI, with 730 and 740 nm emitting pools present (*7*). From the above-mentioned Stepanov (*9*) calculations it would appear that the fluorescence yield of the red forms is similar to that of the bulk antenna chlorophylls. A number of attempts have been made to determine the absorption origin bands of these red emission forms with most suggestions pointing toward absorption bands with maxima near 695, 708, and 716 nm (e.g., refs *15*, *18*). If these suggestions are correct, then the red forms would appear to have very large Stokes shifts (10−25 nm). However it must be pointed out that, when the Stokes shift is determined from an absorption/fluorescence comparison in chlorophyll−protein complexes, as is usually the case, such factors as site inhomogeneous broadening, excitonic pigment interactions, and the presence of low-

* To whom correspondence should be addressed. E-mail: Robert.Jennings@unimi.it.

‡ Present address: Max-Planck Institut für Strahlenchemie, Mülheim a.d. Ruhr, Germany.

[1] Abbreviations: Chl, chlorophyll; DM, *n*-dodecyl-*β*-D-maltoside; fwhm, full width at half-maximum; LHCI, light-harvesting complex of PSI; LHCII, light-harvesting complex of PSII; PS, photosystem; PSI-200, photosystem I with full antenna complement.

10.1021/bi9813227 CCC: $15.00
Published on Web 11/20/1998

energy vibrational bands can greatly complicate interpretation. The Stokes shifts for non-red-shifted chlorophyll a spectral forms in chlorophyll−protein complexes, based on the electron−phonon coupling properties, have been determined to be not greater than 2 nm (*19*, *20*). As the Stokes shift is determined by the homogenoeus bandwidth characteristics, and thus in the final analysis, by the electron−phonon coupling properties of the pigment in its protein binding pocket (Stokes shift $\equiv 2S\nu_m$, where S is the electron−phonon coupling strength and ν_m is the mean host phonon frequency), the very large values suggested may indicate unusually high optical reorganization energies ($S\nu_m$) for red antenna forms (*18*). Absorption hole burning in the red tail of a PSI core particle (*21*) has in fact indicated the presence of chlorophyll with very high optical reorganization energy ($S\nu_m = 200$ cm^{-1}), though it appears that this is due to P700 and not to a red antenna form.

To further study this problem we have used an alternative approach, in which the thermal broadening of the red absorption tail of PSI-200, LHCI, and PSI core was analyzed in terms of the second-order central moment and compared with that of the bulk antenna pigments. This approach was recently demonstrated to yield reliable information for the LHCII absorption band (*20*). The data indicate that $S\nu_m$ for the red tail is at least three times greater than that for the bulk chlorophylls, which is similar to chlorophyll a antenna molecules in other chlorophyll−protein complexes.

MATERIALS AND METHODS

Purification of PSI-LHCI. Leaves of 15-day-old Zea mays were homogenized in 0.4 M sorbitol, 0.1 M Tricine, pH 7.8, 10 mM NaCl, and 5 mM $MgCl_2$. Isolation of the thylakoids was performed as described previously (*22*). Freshly prepared thylakoids were resuspended at 1 mg/mL chl in distilled water and solubilized by *n*-dodecyl-β-D-maltoside (DM) at a final concentration of 1%. After stirring for 20 min at 4 °C, the sample was centrifuged for 10 min at 40000*g*, and 6-mL aliquots of the supernatant were loaded on 0.1−1 M sucrose gradients (35 mL) layered over 2 mL of 2 M sucrose, containing 5 mM Tricine, pH 7.8, and 0.03% DM. After centrifugation for 42 h at 28 000 rpm in a SW28 rotor (Beckman) at 4 °C, four green bands were distinguishable. The bands were collected and analyzed by SDS−PAGE (*23*). The lowermost band, containing PSI-200, was diluted in 5 mM Tricine, pH 7.8, and centrifuged for 3 h at 70000 rpm in an 80 Ti rotor (Beckman). The pellet was resuspended in 5 mM Tricine, pH 7.8, and 50 mM sorbitol, frozen in liquid nitrogen, and stored at −80 °C.

Purification of PSI Core and LHCI. The pellet from PSI-200 preparation was resuspended at 0.3 mg/mL in distilled water and solubilized by 1% DM and 0.5% Zwittergent-16. After stirring for 20 min at 4 °C the sample was rapidly frozen in liquid nitrogen and slowly thawed to improve the detachment between PSI core and LHCI. Samples (1.5 mL-aliquots) were loaded on a 12-mL 0.1−1 M sucrose gradient, also containing 5 mM Tricine, pH 7.8, and 0.03% DM. After centrifugation for 24 h at 4 °C at 41 000 rpm in a SW41 rotor (Beckman), five green bands were obtained. The bands were analyzed by SDS−PAGE (*23*). The second band from the top contained all of the LHCI polypeptides and the third the PSI core particles. The fractions were frozen in liquid nitrogen and stored at −80 °C.

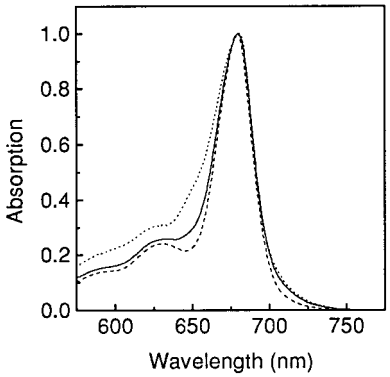

FIGURE 1: Absorption spectra of PSI-200 (solid line), PSI core (dashed line), and LHCI (dotted line) in Tricine 5 mM, pH 7.8, 0.015% DM at 290 K. Spectra have been normalized to the peak value.

Absorption and Fluorescence Spectroscopy. The absorption and fluorescence emission spectra were measured using a EG&G OMAIII (Model 1460) with an intensified diode array (Model 1420) mounted on a spectrograph (Jobin-Yvon HR320) with a 150 groove mm^{-1} grating. The wavelength scale of the instrument was calibrated using a spectral line calibration source (Cathodeon). The absorption spectra were registered as previously reported (*20*). The samples were diluted in a buffer containing Tricine 5 mM, pH 7.8, glycerol 60%, and 0.015% DM.

The fluorescence spectra were recorded as previously described (*7*), but in the presence of 0.015% DM.

The thermal broadening analysis was performed as previously described (*20*).

RESULTS

Absorption and Emission Spectra of PSI-200, LHCI and PSI Core. Steady-state absorption spectra of PSI-200, LHCI, and the PSI core particle are presented in Figure 1. As pointed out in the Materials and Methods section, both core and LHCI preparations are derived from the PSI-200 preparation. To facilitate comparison, all preparations were suspended in the same low concentrations of dodecyl maltoside (0.015%). All preparations display absorption maxima, associated with the bulk antenna chlorophylls, near 680 nm. While this is similar to previously reported data for PSI-200 and core particles (*7*, *22*, *24*) the literature values for LHCI are considerably blue-shifted (*16*, *17*, *25*). We believe that our spectrum for LHCI is close to that of the in vivo complex, as it is possible to successfully describe the PSI-200 spectrum by the equally weighted sum of the present LHCI and core spectra (data not presented). Under these conditions the red wing of PSI-200 is somewhat decreased with respect to that previously reported by us owing to the presence of detergent here (*7*). It is apparent that the red absorption tail is much greater in LHCI with respect to the core prepartion. On the basis of Gaussian decomposition of the LHCI spectrum, in which the red tail is well-described by 3 red forms with maxima near 701, 715, and 726 nm in the 80−300 K temperature range (data not presented), we estimate that the absorption intensity associated with the red forms is between 10% and 12% of the total Q_y absorption in LHCI, whereas this value is about 4% in the core. As part of this is associated with P700 in the core, it can be

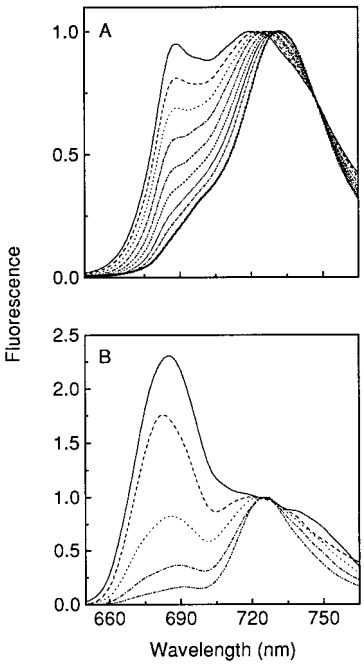

FIGURE 2: Fluorescence spectra of LHCI (A) and PSI core (B) in Tricine 5 mM, pH 7.8, 0.015% DM, and 60% glycerol, measured at different temperatures. Decreasing fluorescence values at 690 nm are associated with decreasing measurement temperatures. In A, the temperatures (in K) are 280, 265, 250, 225, 200, 175, 150, 125, and 80 and spectra are normalized to the maximum. In B, the temperatures (in K) are 280, 225, 175, 125, and 80 with normalization at 725 nm.

shown that the antenna red form content of this particle is probably about 4−5 times less than that in LHCI.

In Figure 2 some steady-state emission spectra for the LHCI and core preparations in the 80−300 K are presented. At 280 K the LHCI emission displays a quite intense emission at 680−690 nm, associated with the bulk antenna, and a prominent red emitting band with a maximum around 720 nm. This latter band shifts to longer wavelengths upon lowering the temperature, with an 80 K emission peak at 732 nm. This temperature-dependent behavior is qualitatively similar to that already reported for our PSI-200 preparation (*7*), though less pronounced, and reflects the expected increased population of the lower-energy states at low temperatures. These data therefore indicate the presence of a number of energetically different red forms in LHCI.

The core emission spectra are markedly different with respect to LHCI. At high temperatures the overall fluorescence yield is low and red form emission is weak, in agreement with previous studies (*6*, *17*). This latter observation supports the above interpretation that the core has a low red form content. In addition the main band, near 725 nm, does not become progressively red-shifted upon lowering the temperature even though the usually observed large increases in fluorescence yield occurred. This may indicate that the isolated core particle contains only a single red form. We have checked whether the relatively intense 680−690 nm emission at high temperatures may be associated with some uncoupled chlorophylls by determining the emission spectrum in the presence of an added quinone quencher of chlorophyll fluorescence (dibromothymoquinone, 2 μM). As the quenching efficiency is the same over the entire emission band (data not presented), uncoupled chlorophylls do not seem to be present.

Thermal Broadening Analysis of Absorption Spectra. It is well-known that the bandwidth for a thermally broadened absorption transition is given by the following (*19*):

$$\sigma_b^2 = \sigma_h^2 + \sigma_i^2 \quad (1)$$

where σ_b^2, σ_h^2, and σ_i^2 are the mean square standard deviations of the total band and the homogeneous and inhomogeneous contributions, respectively.

For linear electron−phonon coupling this can be rewritten (*26*, *27*):

$$\sigma_b^2 = S\nu_m^2 \coth\left(\frac{hc\nu_m}{2kT}\right) + \sigma_i^2 \quad (2)$$

where S is the linear electron−phonon coupling strength, ν_m is the mean phonon frequency (cm^{-1}), T is the absolute temperature, and k, c, and h are fundamental constants. It is usually assumed that σ_i^2 is temperature-independent, though this may not always be the case (*28*).

For a composite absorption band, which in the following will also be called the total absorption band, in which a number N of energetically different transitions are present (heterogeneously broadened) a similar expression can be written (*20*):

$$\sigma_{tot}^2 = \sum_{k=1}^{N} A_k S_k \nu_{mk}^2 \coth\left(\frac{hc\nu_{mk}}{2kT}\right) + \sigma_i^2 \quad (3)$$

where A_k is the absorption intensity weighting factor. In this case σ_i^2 is a complex term describing both the inhomogeneous distribution of the single transitions and the heterogeneous broadening of the composite absorption band (*20*). Thus the temperature sensitive part of the mean square deviation of a composite absorption band (σ_{tot}^2) is given simply by the intensity weighted sum of the σ^2 values of the individual transitions. As the mean phonon frequency (ν_m) for protein-bound chlorophylls has been determined by absorption hole burning to be in the 20−30 cm^{-1} interval (*19*, *21*) eq 3 may be approximated by

$$\sigma_{tot}^2 = 1.39 \sum_{k=1}^{N} A_k S_k \nu_{mk} T + \sigma_i^2 \quad (4)$$

In principle eqs 3 and 4 are also applicable to segments of a composite absorption spectrum.

In the present paper we have used eq 4 to analyze the thermal broadening properties of the heterogeneously broadened spectra of PSI-200, LHCI, and the PSI core, in the Q_y region, to obtain estimates for $S\nu_m$. In the assumption that the electron−phonon coupling characteristics of the underlying transitions of a composite spectral region are similar, plotting σ_{tot}^2 versus T yields the $S\nu_m$ of the single transitions. When this assumption is not upheld this plot gives a kind of average $S\nu_m$ for the various transitions.

In Figure 3 some sample absorption spectra of the PSI-200 and LHCI preparations in the 80−300 K range are shown. Calculations of σ_{tot}^2 were initially performed for the entire spectral band in the wavelength interval above 658 nm (15 200 cm^{-1}) and are plotted as a function of temperature in Figure 4. The integrated areas under the absorption bands were conserved over this temperature interval. All

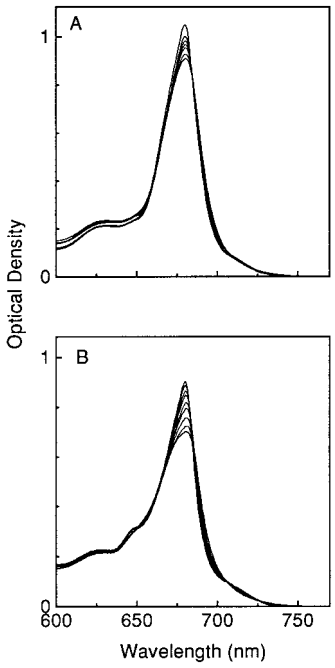

FIGURE 3: Absorption spectra of PSI-200 (A) and LHCI (B) in Tricine 5 mM, pH 7.8, 0.015% DM, and 60% glycerol, measured at different temperatures between 300 and 80 K.

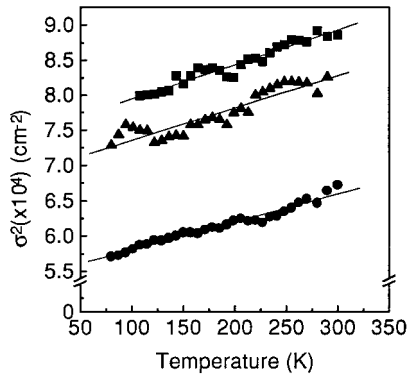

FIGURE 4: The second-order central moment, σ^2, of the PSI-200 (▲), LHCI (■), and PSI core (●) absorption bands determined for the wavenumber interval 13300−15200 cm^{-1} as a function of temperature. The linear fit gives the following: (▲) $S\nu_m = 33$ cm^{-1}, (■) $S\nu_m = 35$ cm^{-1}, (●) $S\nu_m = 28$ cm^{-1}.

data can be described by linear plots, though in the case of PSI-200, there is considerable dispersion. When the slopes are analyzed in terms of eq 4, $S\nu_m$ values of 33, 35, and 28 cm^{-1} are determined for PSI-200, LHCI, and the core, respectively. These values are all somewhat greater than those determined for some PSI bulk chlorophylls by hole burning ($S\nu_m = 20$ cm^{-1}, ref *29*), and as will be seen below, this is due to the presence of the red absorption tail.

One way to analyze the bulk antenna and the red tail separately would be to decompose the absorption spectrum into Gaussian subbands and to calculate the mean square deviation for the two sets of subbands associated with these two spectral regions according to eqs 3 and 4. However, as the PSI preparations contain a very large number of pigment sites, it would be virtually impossible to find a physically meaningful, and hence temperature-stable, subband description in which the subband positions and intensities remain constant over the temperature range used here. We have therefore chosen a second approach in which the absorption

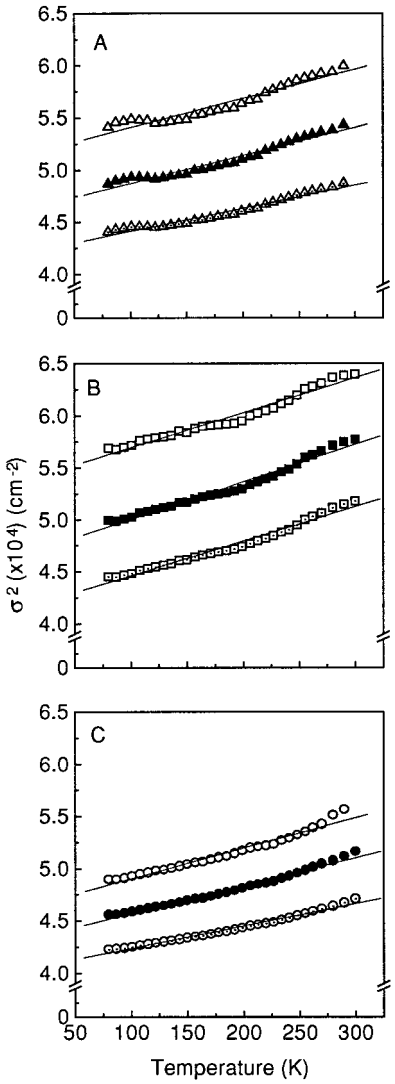

FIGURE 5: The second-order central moment, σ^2, of the bulk absorption band of PSI-200 (A), LHCI (B), and PSI core (C), with different wavelength "cuts" as a function of temperature. For all complexes the open symbols represent the σ^2 calculated in the 14100−15200 cm^{-1} interval, the solid symbols 14200−15200 cm^{-1}, and the open-dot symbols 14300−15200 cm^{-1}. For each complex the three linear fits yield (A) $S\nu_m = 20$ cm^{-1}, $S\nu_m = 19$ cm^{-1}, and $S\nu_m = 16$ cm^{-1}; (B) $S\nu_m = 24$ cm^{-1}, $S\nu_m = 26$ cm^{-1}, and $S\nu_m = 24$ cm^{-1}; and (C) $S\nu_m = 21$ cm^{-1}, $S\nu_m = 19$ cm^{-1}, and $S\nu_m = 15$ cm^{-1}.

spectra were analytically interrupted (cut) at some wavelength. As can be seen from Figure 3 the dividing wavelength region between the bulk antenna and the red tail is around 700 nm. We have therefore "cut" all spectra at 699 (14 300 cm^{-1}), 704 (14 200 cm^{-1}), and 709 nm (14 100 cm^{-1}) and for the bulk antenna have analyzed σ^2, for each complex, in the following three wavelength intervals: 658−699, 658−704, and 658−709 nm. For the red tail σ^2 was determined separately from 699, 704, and 709 nm. In Figure 5 the thermal broadening plots for the bulk chlorophylls for the three above indicated spectral intervals are shown for PSI-200, LHCI, and the core. The data are approximated by a straight line, though in all cases a somewhat regular fluctuation around the linear fit is apparent. Analysis of the linear slope in terms of eq 4 yields $S\nu_m$ values between 15 and 25 cm^{-1}, with the highest values being associated with LHCI. These average values are in quite good agreement

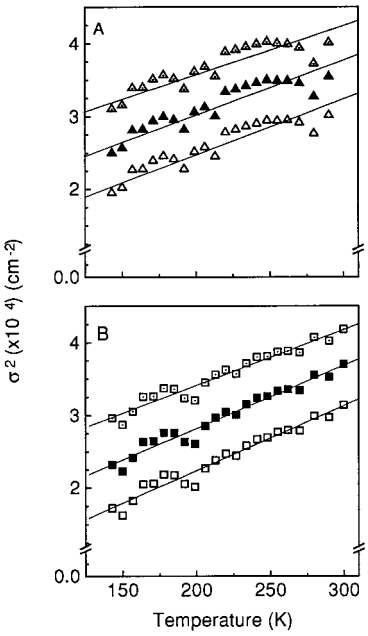

FIGURE 6: The second-order central moment, σ^2, of the red absorption tail of PSI-200 (A) and LHCI (B), with different wavelength "cuts" as a function of temperature. For all complexes the open symbols represent the σ^2 calculated in the 13300−14100 cm^{-1} interval, the solid symbols 13300−14200 cm^{-1}, and the open-dot symbols 13300−14300 cm^{-1}. For each complex the three linear fits yield (A) $S\nu_m = 55$ cm^{-1}, $S\nu_m = 54$ cm^{-1}, and $S\nu_m = 48$ cm^{-1}; and (B) $S\nu_m = 65$ cm^{-1}, $S\nu_m = 62$ cm^{-1}, and $S\nu_m = 55$ cm^{-1}.

with hole burning and show that it is red tail which led to the higher S values for the total band (Figure 4). For the red tail the thermal broadening analysis (Figure 6) was restricted to PSI-200 and LHCI owing to its very low intensity in the core preparation. In both cases area fluctuations between 80 and 300 K were within 5%. In all cases the data are well-described by a linear fit with $S\nu_m$ values in the range 50−65 cm^{-1}. These values are about three times greater than those for the bulk chlorophylls.

DISCUSSION

In the present study the intact photosystem I particle (PSI-200) from maize has been fractionated into its outer antenna components, a mixture of four chlorophyll a/b binding complexes known as LHCI (*30*−*32*), and the core complex. From the absorption and fluorescence spectra it is evident that the red spectral form content is very different for LHCI and the core, with the former containing much higher amounts. In terms of absorption intensity above 700 nm we believe that at least 80% of the red forms are associated with outer antenna complexes. On the basis of our earlier analysis of PSI-200 (*7*) in which a minimum number of three red forms was proposed, associated with 10−12 chlorophyll molecules per photosystem, we therefore suggest that the maximum number of red absorbing antenna pigments in the isolated core is 2/complex. The absence of fluorescence red shifting in the core at low temperatures furthermore suggests that only one spectral form may be present. Thus it is clear that the higher plant photosystem I core has a much lower red form content and energy spread than that of cyanobacteria (e.g., refs *8*, *18*, *33*, *34*) where the intensity of the red tail is rather similar to that described here for LHCI.

We have analyzed the thermal broadening of PSI-200, LHCI, and the core complex absorption spectra in terms of the second-order central moment, as previously described for LHCII (*20*). In the linear electron−phonon coupling assumption this approach yields an average value for the optical reorganization energy ($S\nu_m$) of the absorption transitions lying under the analyzed spectral region. For LHCII, total band values for $S\nu_m$ in the 10−20 cm^{-1} range were found, in good agreement with the limited hole burning data for a single chlorophyll form in that complex (*35*). In the present study essentially similar values were found for the bulk antenna chlorophylls ($S\nu_m = 15-25$ cm^{-1}) which are also in good agreement with hole burning (*29*, *36*). The highest values were associated with the bulk chlorophylls of LHCI ($S\nu_m = 24-25$ cm^{-1}). We therefore conclude (eq 2) that the homogeneously broadened bandwidths (fwhm) associated with the $Q_y(0,0)$ for bulk PSI chlorophylls at room temperature, similar to those for LHCII, are close to 215 cm^{-1} (10 nm) and that the Stokes shifts ($2S\nu_m$) are expected to be about 2 nm.

While the bulk PSI chlorophylls are characterized by electron−phonon coupling properties rather similar to those of other antenna chlorophylls, the red antenna forms, absorbing at wavelengths above 700 nm, are not. Thermal analysis of the red tail after "cutting" the spectrum at different wavelengths yielded $S\nu_m$ values in the 50−65 cm^{-1} interval. The very similar values for the two samples analyzed are not surprising as most of the red forms are in fact associated with LHCI (see Discussion above). This clearly shows that the optical reorganization energy of the red forms is much greater than that of the bulk PSI chlorophylls as well as the antenna chlorophylls of PSII complexes. We point out, however, that the technique of analyzing the "cut" tail in this way will lead to an underestimation of the real $S\nu_m$ value due to (a) the presence of the red wing of bulk chlorophylls in the analyzed region and (b) the elimination of the blue tail of highest-energy red forms. We have therefore used an alternative approach to estimate this parameter. In the assumption that the electron−phonon coupling properties within each of the spectral intervals considered, that is, the bulk and red tail regions, are equal, from eq 3 we may write the following:

$$(S\nu_m)_{tot} = A_b(S\nu_m)_b + A_r(S\nu_m)_r \qquad (5)$$

where A_b and A_r are the absorption weightings of the bulk and red forms respectively, and $(S\nu_m)_{tot}$, $(S\nu_m)_b$, and $(S\nu_m)_r$ are the average reorganization energies of the total absorption band, bulk chlorophylls, and the red forms, respectively. When this approach is applied to LHCI, for which we estimate that the red forms carry about 10−12% (A_r) of the total Q_y intensity, and using the $(S\nu_m)_{tot}$ and $(S\nu_m)_b$ of Figures 4 and 5, we find $(S\nu_m)_r$ 110 cm^{-1}. As the red tail of PSI contains at least 3 spectroscopically identifiable spectral forms (*7*), there may, of course, also be some heterogeneity in the optical reorganization energy.

The present $S\nu_m$ determinations suggest that the bandwidths of red forms may be great, with minimum fwhm values at room temperature for the homogeneously broadened $Q_y(0,0)$ transitions of around 400−500 cm^{-1} (20−25 nm) and Stokes shifts ($2S\nu_m$) in the 6−11 nm range. From the above Discussion we favor the higher values. These values,

while being much greater than those for the bulk antenna chlorophylls, are less than the value of 17 nm suggested by Gobets et al. (*18*), on the basis of site-selected fluorescence measurements, for the lowest-energy transition in PSI-200. They are, however, similar to that suggested by the same authors for the lowest-energy transition in *Synechocystis* core particles (10 nm). The huge Stokes shift found by Gobets et al. (*18*) for the PSI200 red form suggests a reorganization energy of 160 cm^{-1}. The discrepancy with respect to the values which we report here may, of course, be associated with heterogeneity in electron−phonon coupling between the red forms with our values being average ones. On the other hand interpretation of the site-selected fluorescence data assumes that emission is coming from the same transition that is being excited, and this is extremely difficult to demonstrate with any certainty. For example, if the red forms were to be associated with excitonically interacting chlorophylls, very large apparent Stokes shifts could be due to excitation into the high-energy excitonic band with emission originating exclusively from the low-energy transition (*37*) at the very low temperatures (1−2 K) employed in site-selected experiments. In this scenario most of the apparent Stokes shift may be expected to be associated with the excitonic band splitting. However it should be mentioned that absorption hole burning into the red tail of a spinach PSI core particle (burn wavelength near 715 nm) yielded the very high reorganization energy of 200 cm^{-1} (*21*). In view of the only very weak burn wavelength dependence of the hole maxima (between 702 and 705 nm at 1.5 K) and the almost unchanged phonon sideband energy spread, this was associated with P700 and not with an antenna form. The present observation of the paucity of red forms in the PSI core from higher plants lends weight to this view. Thus while available data indicate that the red antenna forms have unusually large reorganization values with respect to non-red-shifted antenna chlorophylls, to date the different approaches used are not in full agreement as to the exact values.

ACKNOWLEDGMENT

This work was in part supported by the “Piano Nazionale Biotecnologie Vegetali”, MIRAAF- Italy.

REFERENCES

1. Mullet, J. E., Burke, J. J., and Arntzen, C. J. (1980) *Plant Physiol. 65*, 814−822.
2. French, C. S., Brown, J. S., and Lawrence, M. C. (1972) *Plant Physiol. 49*, 421−429.
3. Marchiarullo, M. A., and Ross, R. T. (1985) *Biochim. Biophys. Acta 807*, 52−63.
4. Werst, M. M., Jia, Y., Mets, L., and Fleming, G. R. (1992) *Biophys. J. 61*, 868−878.
5. Jia, Y., Jean, J. M., Werst, M. M., Chan, C. K., and Fleming, G. R. (1992) *Biophys. J. 63*, 259−273.
6. Turconi, S., Weber, N., Schweitzer, G., Strotmann, H., and Holzwarth, A. R. (1994) *Biochim. Biophys. Acta 1187*, 324−334.
7. Croce, R., Zucchelli, G., Garlaschi, F. M., Bassi, R., and Jennings, R. C. (1996) *Biochemistry 35*, 8572−8579.
8. Pålsson, L. O., Flemming, C., Gobets, B., van Grondelle, R., Dekker, J. P., and Schlodder, E. (1998) *Biophys. J. 74*, 2611−2622.
9. Stepanov, B. I. (1957) *Sov. Phys. Dokl.* 2, 81−84.
10. van Grondelle, R., Bergström, H., Sundström, V., van Dorssen, R. J., Vos, M., and Hunter, C. N. (1988) in *Photosynthetic Light-harvesting Systems. Organisation and Function* (Scheer, H., and Schneider, S., Eds.) pp 519−530, Walter de Gruyter & Co., Berlin and New York.
11. Fischer, M. R., and Hoff, A. J. (1992) *Biophys. J. 63*, 911−916.
12. Trissl, H. W. (1993) *Photosynth. Res. 35*, 247−263.
13. Jennings, R. C., Zucchelli, G., Croce, R., Valkunas, L., Finzi, L., and Garlaschi, F. M. (1997) *Photosynth. Res. 52*, 245−253.
14. Anderson, J. M. (1982) *Photobiochem. Photobiophys. 3*, 225−241.
15. Wittmershaus, B. P. (1987) in *Progress in Photosynthesis Research*, (Biggins, J., Ed.) pp 75−82, Vol. 1, Martinus Nijhoff Publisher, Dordrecht, the Netherlands.
16. Mukerji, I., and Sauer, K. (1993) *Biochim. Biophys. Acta 1142*, 311−320.
17. Pålsson, L. O., Tjus, S. E., Andersson, B., and Gillbro, T. (1995) *Biochim. Biophys. Acta 1230*, 1−9.
18. Gobets, B., van Amerongen, H., Monshouwer, R., Kruip, J., Rogner, M., van Grondelle, R., and Dekker, J. P. (1994) *Biochim. Biophys. Acta 1188*, 75−85.
19. Hayes, J. M., Gillie, J. K., Tang, D., and Small, G. J. (1988) *Biochim. Biophys. Acta 932*, 287−305.
20. Zucchelli, G., Garlaschi, F. M., and Jennings, R. C. (1996) *Biochemistry 35*, 16247−16254.
21. Gillie, J. K., Lyle, P. A., Small, G. J., and Golbeck, J. H. (1989) *Photosynth. Res. 22*, 233−246.
22. Bassi, R., and Simpson, D. J. (1987) *Eur. J. Biochem. 163*, 221−230.
23. Bassi, R., Hoyer-Hansen, G., Barbato, R., Giacometti, G. M., and Simpson, D. J. (1987) *J. Biol. Chem. 262*, 13333−13341.
24. Dunahay, T. G., and Staehelin, L. A. (1985) *Plant Physiol. 78*, 606−613.
25. Tjus, S. E., Roobolboza, M., Pålsson, L. O., and Andersson, B. (1995) *Photosynth. Res. 45*, 41−49.
26. Lax, M. (1952) *J. Chem. Phys. 20*, 1752−1760.
27. Stepanov, B. I., and Gribkovskii, V. P. (1968) *Theory of Luminescence*, ILIFFE Books Ltd., London.
28. Ormos, P., Ansari, A., Braunstein, D., Cowen, B. R., Frauenfelder, H., Hong, M. K., Iben, I. E. T., Sauke, T. B., Steinbach, P. J., and Young, R. D. (1990) *Biophys. J. 57*, 191−199.
29. Gillie, J. K., Small, G. J., and Golbeck, J. H. (1989) *J. Phys. Chem. 93*, 1620−1627.
30. Jansson, S. (1994) *Biochim. Biophys. Acta 1184*, 1−19.
31. Jennings, R. C., Bassi, R., and Zucchelli, G. (1996) in *Topics in Current Chemistry, 177*: *Electron-Transfer II* (Mattay, J., Ed.) pp 147−181, Springer-Verlag, Berlin and Heidelberg, Germany.
32. Jansson, S., Stefansson, H., Nyström, U., Gustafsson, P., and Albertsson, P. A. (1997) *Biochim. Biophys. Acta 1320*, 297−309.
33. Shubin, V. V., Bezsmertnaya, I. N., and Karapetyan, N. V. (1995) *J. Photochem. Photobiol., B*: *30*, 153−160.
34. Koehne, B., and Trissl, H. W. (1998) *Biochemistry 37*, 5494−5500.
35. Reddy, N. R. S., van Amerongen, H., Kwa, S. L. S., van Grondelle, R., and Small, G. J. (1994) *J. Phys. Chem. 98*, 4729−4735.
36. Gillie, J. K., Hayes, J. M., Small, G. J., and Golbeck, J. H. (1987) *J. Phys. Chem. 91*, 5524−5527.
37. Davydov, A. S. (1971) *Theory of Molecular Excitons*, Plenum Press, New York.

BI9813227